

LA-UR- 10-04838

Approved for public release;  
distribution is unlimited.

*Title:* Performance of Commercial Off-The-Shelf Microelectromechanical Systems Sensors in a Pulsed Reactor Environment

*Author(s):* Keith E. Holbert, A. Sharif Heger, Steven S. McCready

*Intended for:* IEEE Nuclear and Space Radiation Effects Conference, July 2010, Denver, Colorado



Los Alamos National Laboratory, an affirmative action/equal opportunity employer, is operated by the Los Alamos National Security, LLC for the National Nuclear Security Administration of the U.S. Department of Energy under contract DE-AC52-06NA25396. By acceptance of this article, the publisher recognizes that the U.S. Government retains a nonexclusive, royalty-free license to publish or reproduce the published form of this contribution, or to allow others to do so, for U.S. Government purposes. Los Alamos National Laboratory requests that the publisher identify this article as work performed under the auspices of the U.S. Department of Energy. Los Alamos National Laboratory strongly supports academic freedom and a researcher's right to publish; as an institution, however, the Laboratory does not endorse the viewpoint of a publication or guarantee its technical correctness.

# Performance of Commercial Off-The-Shelf Microelectromechanical Systems Sensors in a Pulsed Reactor Environment

Keith E. Holbert, *Senior Member, IEEE*, A. Sharif Heger, Steven S. McCready

**Abstract**—Prompted by the unexpected failure of piezoresistive sensors in both an elevated gamma-ray environment and reactor core pulse tests, we initiated radiation testing of several MEMS piezoresistive accelerometers and pressure transducers to ascertain their radiation hardness. Some commercial off-the-shelf sensors are found to be viable options for use in a high-energy pulsed reactor, but others suffer severe degradation and even catastrophic failure. Although researchers are promoting the use of MEMS devices in radiation-harsh environment, we nevertheless find assurance testing necessary.

**Index Terms**—microelectromechanical devices, nuclear radiation effects, piezoresistive devices, transducers.

## I. INTRODUCTION

CONDUCTING a systems test in a high-energy pulsed reactor can pose several instrumentation problems. Transducers intended for measuring properties such as temperature, pressure, and acceleration can be damaged by exposure to the radiation, or they may be affected by the radiation such that measurement error is introduced. When selecting transducers such factors must be considered together with requirements related to preventing the sensor presence from perturbing the system under study. In addition, pulsed radiation can induce current into the sensing cables [1].

We present total dose testing of several microelectromechanical systems (MEMS) accelerometers and pressure transducers to ascertain their radiation hardness after piezoresistive sensors failed unexpectedly in an elevated gamma-ray environment and reactor core pulse tests. Such instrumentation is attractive to reactor experiments due to their small size and broad range of frequency response. The overall goal of this study is to assess the usefulness of commercial off-the-shelf (COTS) sensors for experiments, especially shock testing, taking place in a pulsed reactor core.

## II. BACKGROUND

Since the primary focus of this paper is reporting the performance of COTS MEMS piezoresistive sensors in the pulsed reactor environment, we dedicate this background section to understanding the operation of MEMS piezoresistive sensors and to surveying prior research into radiation effects on such devices.

### A. Piezoresistive MEMS Sensors

In 1954 Smith reported on the piezoresistance effect in germanium and silicon [2]. In the late 1950s and early 1960s, silicon strain gages were commercialized. Silicon pressure transducers were developed in the 1960s into the 1970s. The first piezoresistive silicon accelerometer was reported in 1979 [3]. Piezoresistive accelerometers are essentially semiconductor strain gages possessing large gage factors since the material resistivity primarily depends on the stress rather than the dimensions [4]. These micromachined accelerometers using a piezoresistive detection principle are mainly used in automotive applications [5], but have also been used in space applications [6]. In the case of MEMS accelerometers, several transducer concepts are in use including piezoresistive, piezoelectric, variable capacitance, and force rebalance [7].

Piezoresistive transducers often consist of four resistors arranged in a Wheatstone bridge circuit. The variation of resistivity with strain is then exploited to obtain an output signal proportional to an input force. In a pressure transducer, the resistors are integrated into a diaphragm; for example, Fig. 1 shows the sensing chip of the Kulite pressure transducers tested in this work. For an accelerometer, the resistors are incorporated into the supports for a mass; for instance, the construction of the Endevco accelerometer internals is shown in Fig. 2. In the pressure and acceleration transducers tested in this work, all four arms of the bridge are within the device, but are not necessarily active. An alternative, common design is to include two of the resistors on the sensing element in a “half bridge” arrangement with the other two reference resistors being placed in an external portion of the circuit. Another variation incorporates additional resistors on the sensing element to compensate for the temperature dependence of the sensing material resistivity.

The Kulite pressure transducer utilizes a silicon-on-

Manuscript received July 16, 2010. This work was supported by the U.S. Department of Energy under contract W-7405-ENG-36.

K. E. Holbert is with Arizona State University, Tempe, AZ 85287-5706 USA (phone: 480-965-3424; fax: 480-965-3837; email: holbert@asu.edu).

A. S. Heger and S. S. McCready are with Los Alamos National Laboratory, PO Box 1663, Los Alamos, NM 87545 USA.

insulator (SOI) process, which is thoroughly documented in [8]. The SOI process is beneficial to device design as it allows for complete isolation of the active areas of the device from the silicon substrate. This effectively prevents any problems due to photocurrents from ionizing radiation or even an electromagnetic pulse, and has proven a viable technology in radiation-hard device design. The structure of the Kulite pressure transducer resembles that shown in Fig. 1 [9]. The operation of this device is as follows. Four piezoresistive sensing elements atop the silicon wafer are arranged in a Wheatstone bridge circuit. An applied pressure at the top of the sensor bends the diaphragm, inducing a stress in the piezoresistors on top. The stress is proportional to the difference between the applied pressure and the reference pressure of the isolated aperture beneath the wafer. Applied pressure causes the outer piezoresistors to be placed in tension and the inner piezoresistors to be in compression; the outer two resistors are on opposite sides of the Wheatstone bridge as are the inner two resistors. The supporting member at the bottom has a twofold purpose—it provides mechanical stability for the transducer, as well as forms the sealed cavity underneath the sensing device.

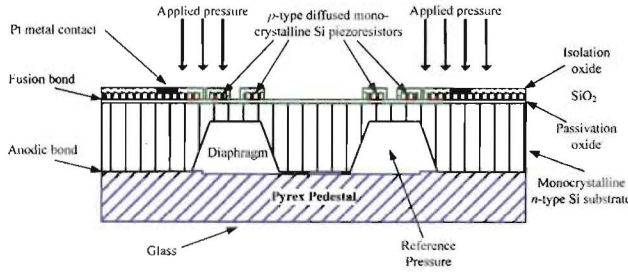


Fig. 1. Kulite piezoresistive pressure transducer construction, adapted from [9]. Applied pressure induces stress in the four piezoresistors, which are arranged in a Wheatstone bridge configuration.

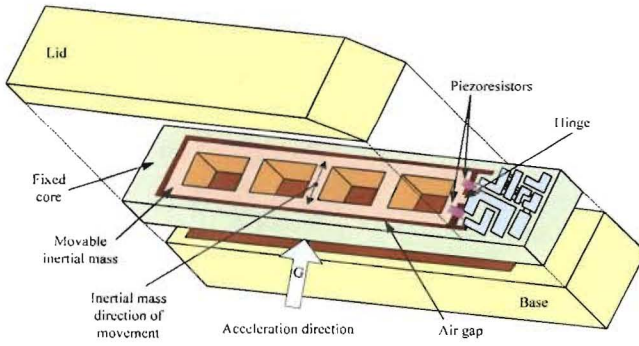


Fig. 2. Completed Endevco accelerometer device, adapted from [10]. The two piezoresistors are located on opposite sides of the hinge and they traverse the air gap between the fixed core and movable inertial mass. Acceleration-induced force on the movable central mass produces tensile and compressive stress, respectively, in the two piezoresistors.

Endevco utilizes a bulk micromachining technique on a silicon wafer to produce the cantilever-type accelerometer depicted in Fig. 2 [10]. The *p*-type silicon piezoresistors are formed by boron diffusion, and they are surrounded by a  $\text{SiO}_2$  layer. The two serpentine-shaped piezoresistive gage

elements extend over the gap; their distance from the hinge controls the sensitivity and range of the sensor. The operation of the particular device shown in Fig. 2 is as follows. The inertial mass is free to move in a direction normal to the central hinge that connects the inertial mass to the fixed core of the accelerometer. This allows acceleration in the force-sensitive direction to induce a stress in the piezoresistors—one piezoresistor is placed in tension and the other in compression. The piezoresistors are placed in adjacent arms of a half-active Wheatstone bridge with  $500 \Omega$  fixed resistors in the other (passive) half of the bridge.

### B. Radiation Effects on MEMS Sensors

Compared to radiation effects studies on conventional technologies, sparse research has been performed to determine the effects of radiation on MEMS devices, particularly those that employ piezoresistors. Since MEMS devices are fabricated in a manner similar to present semiconductor electronics, they are expected to be susceptible to the same types of radiation damage.

Researchers have noted that there is little scientific literature on radiation effects in MEMS and that the field is in its infancy [11,12,13]. Although specific results from radiation testing of MEMS devices is very limited, scientists tout the use of MEMS in radiation environments based on extending their understanding of radiation effects on semiconductor devices to MEMS. For example, the advantage of using MEMS-based satellites due, in part, to their high resistance to radiation was noted in [14,15,16]. A few papers have reported on radiation effects to non-sensor applications of MEMS. Schanwald et al. found that the radiation sensitivity of ground MEMS comb drives and microengines to be approximately  $10^{14}$  electrons/cm<sup>2</sup> ( $\sim 100$  kGy  $\text{SiO}_2$ ) [11]. McClure et al. reported on radiation effects on MEMS radio frequency relays [17]. Caffey and Kladitis report on the effects of photon irradiation of actuators [18]. Miyahira et al. examined the effects of gamma radiation on MEMS optical mirrors [19].

In the 1990s, a few researchers reported on radiation effects in two MEMS accelerometers [20,21,22]. These references describe radiation testing of capacitance type MEMS sensors—the Analog Devices ADXL50 and the Motorola XMMAS40G. Reference [20] found that exposure to protons and heavy ions caused changes in the output voltage due to charge generation, which altered the electric field distribution. In addition, exposure of the ADXL50 to a 250 Gy(Si) gamma dose, created a hysteresis effect at zero *g* where the device appeared to become stuck [21,23]. Boyadzhyan and Choma report on a tunneling accelerometer that was not affected by a 1 kGy gamma dose from Co-60 [24].

More recently, Zhu et al. fabricated one polycrystalline and two silicon-on-insulator (SOI) piezoresistive pressure sensors [25]. They found that a gamma dose of 23 kGy( $\text{H}_2\text{O}$ ) caused a slight shift ( $\sim$  a few mV) in the offset voltages of the three sensors, but no degeneration of linearity or sensitivity.

Because of the limited scientific literature concerning

radiation testing of MEMS devices, information regarding radiation testing of piezoresistive sensors in general (not specifically MEMS) was sought. The findings within the literature are summarized in Table I.

TABLE I  
PIEZORESISTIVE SENSOR RADIATION TESTING RESULTS IN THE LITERATURE

Sensor Type	Radiation Exposure	Key Findings	Reference and Date
Semiconductor strain-gage pressure transducers	$10^{15}$ n/cm <sup>2</sup> and 10 kGy(C) of gamma	Less than 1% change in sensitivity	Terry et al. 1965 [30]
Piezoresistive accelerometers	$6 \times 10^{15}$ n/cm <sup>2</sup> and 3 MGy(C) gamma	Satisfactory dynamic performance; significant changes in unstrained resistance	Chapin et al. 1966 [31]
Piezoresistive accelerometers (18)	$5 \times 10^{15}$ n/cm <sup>2</sup> in TRIGA reactor	Satisfactory operation; negligible to drastic change in strain resistance	Langdon et al. 1970 [26]
Polysilicon and SOI pressure sensors	<sup>60</sup> Co $\gamma$ -rays; dose of 23 kGy(H <sub>2</sub> O)	Sensitivity and linearity did not degenerate; offset voltage shift	Zhu et al. 2001 [25]

Langdon et al. described combined neutron and gamma irradiation testing of two models of piezoresistive accelerometers employing a strain gage element; however, their work was reported in 1970, which was essentially pre-MEMS [26]. They exposed 18 accelerometers to neutron fluences as high as  $5 \times 10^{15}$  epithermal n/cm<sup>2</sup> in a TRIGA reactor (the concomitant gamma dose was unspecified). In that testing, the resistance of an unnamed accelerometer, using unbonded piezoresistive gages that were probably moderately doped, increased dramatically due to the neutron dose. Another manufacturer's model utilizing bonded semiconductor strain gages, which likely were highly doped, operated satisfactorily at all neutron exposures and the gage resistance showed no significant change.

Bouche [27], Thomas [28], and Bierney [29] discuss the design of piezoresistive and piezoelectric accelerometers for operation in nuclear reactor environments. Each of these three Endevco authors cites two other less-accessible company publications dealing with piezoresistive sensor test results: (1) a 1965 Phillips Petroleum Company report by Terry et al. [30], and (2) a 1966 Battelle report by Chapin et al. [31]. Terry et al. exposed semiconductor strain-gage pressure transducers to  $10^{15}$  n/cm<sup>2</sup> and 10 kGy(C) of gamma radiation with less than 1% change in sensitivity. Chapin et al. exposed piezoresistive accelerometers to  $6 \times 10^{15}$  n/cm<sup>2</sup> and 3 MGy(C) of gamma radiation with the sensors exhibiting satisfactory dynamic performance but undergoing significant changes in unstrained resistance. Thomas states that heavily doped gages are far more resistant to reactor radiation effects since the radiation damage mechanism involves changes in the crystalline lattice structure [28].

### III. PULSED REACTOR TESTING AND RESULTS

The tested sensors were operated in the pulsed reactor environments of the Sandia Pulse Reactor (SPR-III) and/or the Annular Core Research Reactor (ACRR) located at Sandia National Laboratories (SNL), NM. Initial testing in the SPR-III provided a smaller ratio of gamma-to-neutron radiation and shorter pulse widths as compared to the ACRR. The ACRR provides pulse-integrated radiation of about a factor of ten larger than the SPR-III, and the ACRR irradiation cavities can accommodate physically larger experiments.

#### A. Pulsed Reactor Characteristics

The SPR-III is a Godiva-type, fast neutron reactor providing a unique, near-fission-spectrum radiation environment (see Table II). SPR-III produces intense neutron bursts for radiation effects testing of materials and electronics. SPR-III has a 17-cm (diameter) central irradiation cavity that extends through the core [32]. The reactor is operated in two basic modes: (1) short duration steady state at low power (10 kW), and (2) fast pulses (bursts).

TABLE II  
NOMINAL PULSE OPERATING PARAMETERS OF THE SPR-III AND ACRR [32]

Characteristic	SPR-III	ACRR
Pulse Yield	11 MJ	300 MJ
Peak Power	$1.5 \times 10^5$ MW	$3.0 \times 10^4$ MW
Pulse Width (FWHM)	76 $\mu$ s	7.0 ms
Peak Gamma Dose Rate	15 MGy(Si)/s	3 MGy(Si)/s
Peak Neutron Flux	$8.0 \times 10^{18}$ n/cm <sup>2</sup> ·s	$6.0 \times 10^{17}$ n/cm <sup>2</sup> ·s
Gamma Dose	1.7 kGy(Si)	30 kGy(Si)
Total	$6.1 \times 10^{14}$ n/cm <sup>2</sup>	$6.0 \times 10^{15}$ n/cm <sup>2</sup>
Neutron	$> 10$ keV	$6.1 \times 10^{14}$ n/cm <sup>2</sup>
Fluence	1 MeV (Si equivalence)	$3.9 \times 10^{15}$ n/cm <sup>2</sup>
	$5.4 \times 10^{14}$ n/cm <sup>2</sup>	$2.8 \times 10^{15}$ n/cm <sup>2</sup>

The ACRR is a pool-type reactor capable of pulsed (see Table II), steady-state and tailored-transient operation [32]. The internal diameter of the ACRR dry central irradiation cavity is 23 cm. In addition, a fuel-ringed external cavity (FREC) is available with a larger diameter of 51 cm for FREC-II [33]. Kelly et al. discuss simulation fidelity issues and compare the radiation environments of the SPR-III and the ACRR (including the FREC) in [34].

#### B. Pulsed Reactor Experiments

The seven reactor experiments, which were carried out over a four-year period, are summarized in Table III. Each pulse within Experiments 2, 3 and 4 was of nearly identical magnitude; the magnitudes of consecutive pulses in Experiments 5, 6 and 7 were systematically increased from  $\sim 30$  to  $\sim 275$  MJ. A brief description of each experiment and the exposed sensors is given in the remainder of this section. The tested sensors were not specifically designed for radiation environments; rather they were COTS devices. For added details on these experiments, the reader is directed to [35].

TABLE III  
PULSED REACTOR TESTING OF MEMS PIEZORESISTIVE SENSORS

Ex- peri- ment	Experiment Description	Total Exposure		MEMS Sensors (model number)
		Gamma (kGy)	Neutron (n/cm <sup>2</sup> )	
1	SPR-III (1 pulse)	1.7	$6.1 \times 10^{14}$	One pressure trans- ducer (Kulite CT-190)
2	SPR-III (4 pulses)	6.8	$2.4 \times 10^{15}$	Two pressure trans- ducers (Kulite XCE- 062 and XTE-190)
3	ACRR (2 pulses)	18	$3.4 \times 10^{15}$	Two pressure trans- ducers (XCE-062 and XTE-190); Two accel- erometers (Endevco 7264C and 7270A)
4	ACRR (5 pulses)	44	$8.7 \times 10^{15}$	One pressure trans- ducer (reused XTE- 190); Two acceler- ometers (7264B)
5	ACRR (3 pulses)	37	$7.4 \times 10^{15}$	Two pressure trans- ducers (XTE-190)
6	ACRR (4 pulses)	55	$1.1 \times 10^{16}$	Two pressure trans- ducers (XTE-190)
7	ACRR (4 pulses)	55	$1.1 \times 10^{16}$	Two pressure trans- ducers (XTE-190)

#### 1) Experiment # 1

During February 2000, the first experiment was performed at the SPR-III. During that test, one Kulite pressure transducer model number CT-190-25A and a Taber strain gage-based pressure transducer (model 2215) were utilized. The Kulite CT-190 is similar to the XTE-190, except that the CT-190 is designed for cryogenic applications with an operating temperature range of  $-320^{\circ}\text{F}$  to  $250^{\circ}\text{F}$ . The two sensors were measuring the pressures of different volumes. The two pressure sensors and a thermistor survived the 11-MJ SPR-III pulse as seen in Fig. 3. No other conclusions can be drawn from this test aside from the fact that both the Kulite and Taber pressure transducers survived on a non-quantitative basis.

Referring to Fig. 3, note that all three sensors exhibit a prompt (impulse-like) change at the time of the reactor pulse. The Kulite pressure transducer is a MEMS device relying on resistance changes as the sensing methodology, whereas the Taber is a strain gage-based pressure transducer. Recall that a thermistor has an inverse (and nonlinear) relationship between its resistance and the sensed temperature. All three responses are consistent with the data acquisition system perceiving a decrease in the resistance of each sensor. The fact that all three sensors exhibit similar response to the reactor pulse appears indicative of a common factor, which might be induced charge/current, and/or cable effects. In other words, the recorded temperature and pressure readings during the actual pulse are artifacts of the reactor pulse originating from radiation-induced signals.

#### 2) Experiment # 2

Also in February 2000, a series of four SPR-III bursts were produced for pressure transducer evaluation. The experiment included a Kulite XCE-062 and an XTE-190, whose use was favored by Los Alamos National Laboratory personnel based on their small size and prior experience (1970s) with the

Kulites in the ACRR. These tests incorporated one Teledyne Taber model 2215 strain gage-based pressure transducer too. Use of the Taber was promoted by SNL personnel because of their experience with those transducers. All three sensors were connected the same volume. The two Kulite pressure transducers qualitatively showed no noticeable degradation to the four reactor pulses, although quantitative comparisons of before and after calibration data were not performed. The Taber pressure sensor also fared well in the testing. These three pressure sensors survived an approximate total neutron fluence of  $2.4 \times 10^{15} \text{ n/cm}^2$  and gamma dose of 6.8 kGy.

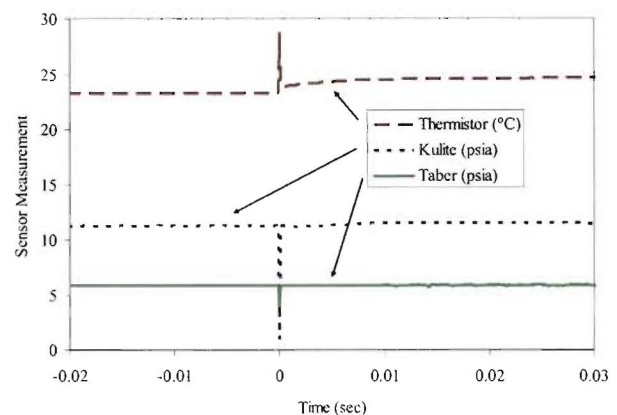


Fig. 3. Thermistor and pressure transducer response to an 11-MJ pulse at  $t=0$  during SPR-III test. The responses of the Kulite and Taber pressure transducers exhibit initial prompt drops, followed a slight increase in steady-state pressure corresponding to the increased pressure.

#### 3) Experiment # 3

In September 2001, a larger scale experiment was conducted in the fuel-ringed external cavity (FREC-II) of the ACRR. The sensors were consecutively subjected to the radiation fields created by two reactor pulses, which were conducted about 90 minutes apart. The two MEMS pressure transducers and two MEMS piezoresistive accelerometers were contained within an aluminum canister.

The time responses of the two Kulite piezoresistive pressure transducers of Experiment 3 are shown in Fig. 4. The pressure transducers respond as showing a peak that is coincident with the reactor pulse; the XCE-062 and the XTE-190 exhibit a negative and a positive response, respectively, to the pulse. These sensor outputs during the pulse are most likely from radiation-induced current and/or system generated electromagnetic pulse (SGEMP) into the sensor cabling. The XCE-062, however, exhibits anomalous behavior immediately after the pulse; specifically, its output returns to a near zero value and then wavers rather than reaching a constant steady-state value as it should. This Kulite XTE-190, which shows no such anomalous behavior, was used later in Experiment 4 where it was exposed to five additional ACRR pulses.

#### 4) Experiment # 4

In May 2002, another sensor evaluation experiment was conducted in the ACRR central cavity. The test consisted of five reactor pulses delivered with approximately one-half hour

of rest between shots. Important to note is that decay heat generation causes the reactor to continue to operate at significant power for two seconds following a high intensity pulse. Each pulse in this experiment involved an energy release of approximately 87 MJ with a peak reactor power of 1200 MW. An 87-MJ ACRR pulse delivers about the same fluence and dose in the central cavity as a 285 MJ pulse delivers in the FREC-II; however, the larger (285 MJ) pulse has a shorter FWHM pulse duration than the smaller (87 MJ) pulse (in general, as the pulse magnitude becomes larger, the full-width half-maximum becomes shorter). Although Fig. 5 only shows data from the first of five reactor pulses, the data for the four other reactor shots are similar and indicate satisfactory operation of the three MEMS-type piezoresistive devices.

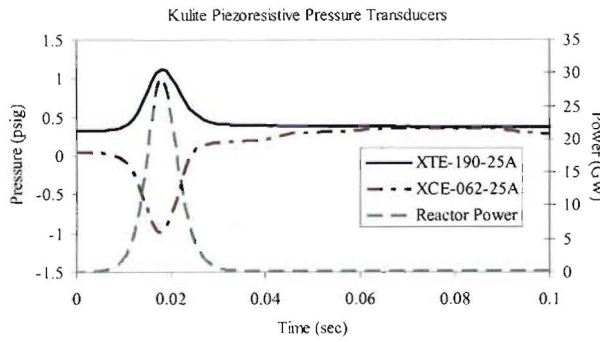


Fig. 4. Kulite piezoresistive pressure transducer outputs vs. time after a 285-MJ ACRR pulse. The initial prompt jump and drop, respectively, by the XTE-190 and XCE-062 outputs are a radiation-induced effect. After the reactor pulse, the XCE-062 exhibits anomalous behavior in terms of a non-constant steady-state output.

For Experiment 4, a solenoid with a spring-loaded piston was mounted inside the test package to perturb the accelerometers while they were in the reactor. Energizing or de-energizing the solenoid produced a single impulse. Solenoid operation consisted of energizing the device, and then waiting about a second, followed by de-energizing the solenoid. This arrangement allowed non-zero stimulation of the accelerometers, but the arrangement was subject to variability and the results should be viewed as qualitative in nature. Solenoid operation is reflected in intermittent peaks in the accelerometer data of Fig. 6. The peaks associated with energizing the solenoid are smaller than those associated with de-energizing it. The oscillations present in the accelerometer data two seconds after the pulse are most likely the result of reactor control rod chain-drive operation. Notice that the accelerometer post-pulse outputs are biased from their pre-pulse zero acceleration values. Specifically, the test results show that one 7264B exhibits a slightly positive (+1.5 g) offset after the reactor shot, whereas the second 7264B has a slightly negative (-0.9 g) offset. The output of each sensor changes over the first few seconds after the reactor shot due to heating of the sensor. Note that although the Wheatstone bridge compensates for identical resistance changes in each bridge leg, the individual piezoresistors are not of identical

resistance ( $R$ ), thereby causing differences in  $\Delta R$  in each leg from temperatures changes.

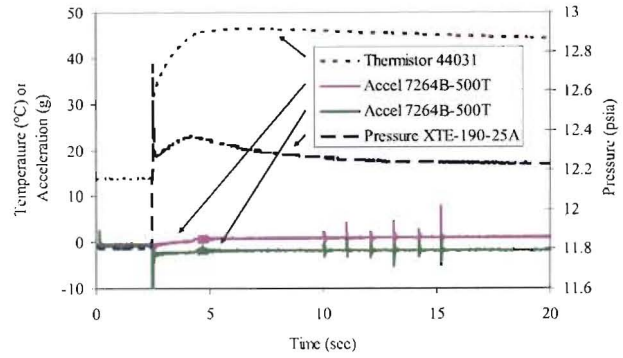


Fig. 5. Sensor outputs from reactor pulse (shot) 1 of Experiment 4. The 87-MJ ACRR pulse occurs at  $t=2.5$  sec, after which temperature and pressure increases are recorded by the instruments.

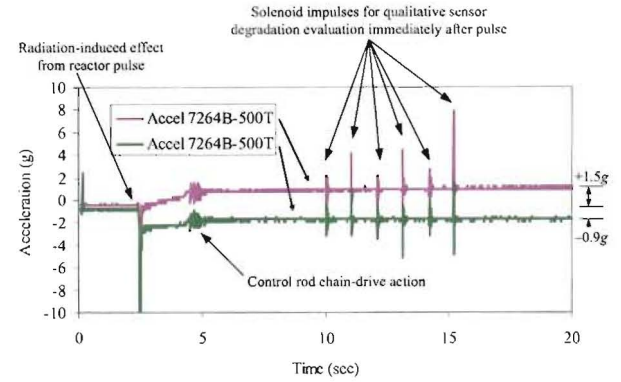


Fig. 6. Endevco 7264B piezoresistive accelerometer outputs following an 87-MJ ACRR pulse at  $t=2.5$  sec. Both accelerometers exhibit a slightly biased output because of the temperature increase.

##### 5) Experiments # 5, 6 and 7

These three experiments were carried out in the ACRR central cavity during September 2003. Three instrumented canisters were placed in the reactor central cavity and subjected to three or four reactor pulses as outlined in Table IV. Two Kulite XTE-190 series pressure transducers were located on the top flange of each aluminum test canister.

Eventually all but one of the six XTE-190 pressure transducers degraded or failed from the total combined gamma dose and neutron fluence, that is, the sensors gradually and systematically deteriorate as the total exposure is increased. For example, Fig. 7 shows that for the first two pulses, the pressure transducer exhibits a normal response to the reactor shots; however, after the third pulse, the sensor begins to display an erratic output, and after the fourth pulse, the magnitude of the erratic behavior has increased noticeably. Other Kulite XTE-190s catastrophically failed after multiple pulses in these experiments. Noteworthy is that the total dose and fluence to the XTE-190s from these experiments are larger than those experiments reported earlier in this paper (see Table III). For comparison, the XTE-190s were found to

fail in a pure gamma environment at doses on the order of 100

kGy [36].

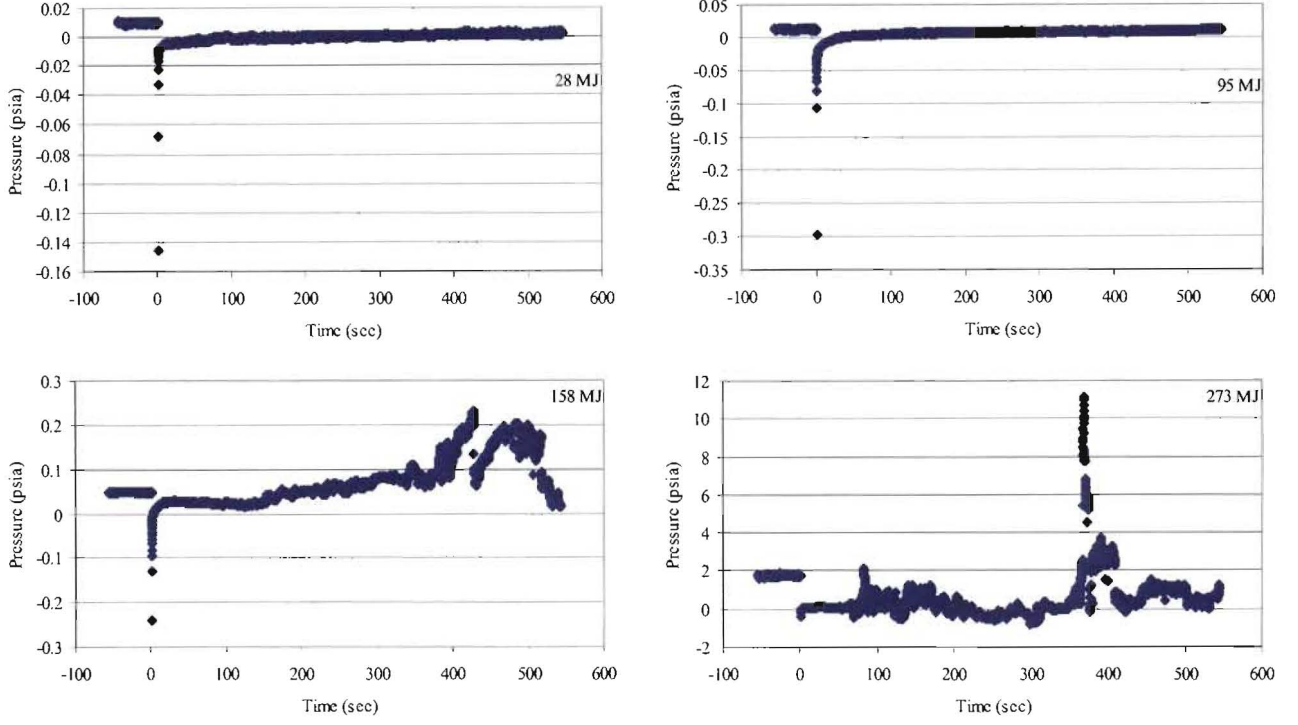


Fig. 7. Degradation of a Kulite XTE-190-25A MEMS pressure transducer for four successively larger ACRR pulses during Experiment 6.

TABLE IV  
REACTOR PULSES IN EXPERIMENTS 5, 6 AND 7

Experiment	Reactor Pulse Energies
5	22 MJ, 78 MJ, 272 MJ
6	28 MJ, 95 MJ, 158 MJ, 273 MJ
7	38 MJ, 81 MJ, 151 MJ, 277 MJ

#### IV. DISCUSSION OF TESTING RESULTS

This section examines the pulsed reactor testing results with respect to the two different sensor types. The piezoresistive sensors tested consist of three different Kulite Semiconductor Products, Inc. pressure transducers (models CT-190, XCE-062 and XTE-190) and two Endevco Corporation accelerometers (models 7264 and 7270A). The Kulite pressure transducers are micromachined silicon-on-insulator (SOI) devices with layers of  $\text{SiO}_2$  sandwiched between adjacent piezoresistive segments, as seen in Fig. 1. The Endevco accelerometers are bulk silicon devices in which the piezoresistive elements extend over an etched hinge for force measurement (see Fig. 2) and are protected by a thin  $\text{SiO}_2$  layer. These sensors are small devices with the piezoresistive elements placed on two or four legs of a Wheatstone bridge. The pressure transducers employ an off-chip thin-film resistive network for temperature compensation whereas the accelerometers do not.

##### A. MEMS Pressure Transducers

The pressure transducers received the greatest attention

during this project with at least one pressure transducer tested in each of the seven experiments. The initial testing in the SPR-III provided a smaller ratio of gamma to neutron radiation as compared to the ACRR. An XCE-062 pressure transducer and an XTE-190 pressure sensor were subjected to four pulses from the SPR-III. In addition, a CT-190 pressure transducer (which is similar to the XTE-190 pressure sensor, except that the CT-190 is designed for cryogenic applications) was exposed to a single SPR-III pulse. These three pressure transducers survived those reactor pulses without observable degradation. Subsequent tests at the ACRR demonstrated another XTE-190 to survive seven pulses (Experiments 3 and 4); however, an XCE-062 exhibited anomalous behavior from a single ACRR pulse. The main difference between the two sensors is their mass: the XCE-062 weighs 0.2 g whereas the XTE-190 has a mass of 4 g [37]. Further exposure to a sustained gamma field resulted in complete failure of the XCE-062 sensor, whereas the XTE-190 continued to function properly, indicating that the XCE-062 is more gamma sensitive. Consequently, the XCE-062 was removed from further consideration.

Six additional XTE-190 transducers were exposed to multiple ACRR pulses in the last three experiments, which showed that for total combined dose and fluence of more than 15 to 25 kGy and  $3 \times 10^{15}$  to  $5 \times 10^{15}$   $\text{n/cm}^2$ , respectively, that most sensor outputs become erratic. Fig. 8 shows a summary of the pressure transducer performance from all seven

experiments. This graph provides users with the capability to predict the survivability of a sensor for an expected dose and fluence in future pulsed reactor experiments.

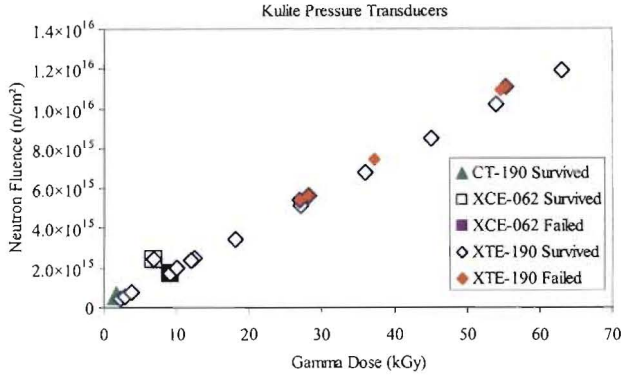


Fig. 8. Post reactor pulse performance of Kulite piezoresistive MEMS pressure transducers. No failures of the XTE-190 are observed below a combined gamma dose of 20 kGy and neutron fluence of  $3 \times 10^{15}$  n/cm<sup>2</sup>.

#### B. MEMS Accelerometers

The Endevco piezoresistive MEMS accelerometers were subjected to pulses from the ACRR only. Fig. 9 shows that the sensors demonstrate a negative pulse coincident with the reactor pulse. The negative pulse is a radiation effect within the sensing elements and/or lead wires versus a physical acceleration. The 7270A shows substantial bias (about  $-107\text{g}$ ) immediately following exposure to a single ACRR pulse; therefore, it was eliminated for use in future pulsed reactor experiments. In contrast, during Experiments 3 and 4, one Endevco 7264C and two 7264B accelerometers were exposed to two and five pulses, respectively, without any noticeable degradation. The 7264C is virtually identical to the 7264B, except that the seismic mass of the 7264C extends from the end of the sensor housing; the resulting difference is that the 7264B has a mounted resonance frequency of 28 kHz and a damping ratio of 0.005, whereas for the 7264C these specifications are 26 kHz and 0.05, respectively. Such comparative values appear to make the 7274B more suitable for the measurement of short duration shocks.

In a prior work, we found that gamma irradiation of these MEMS accelerometers causes the formation of oxide and interface trapped hole charges, which reduce current flow through the piezoresistors due to the creation of a depletion region about the periphery of the gage resistors [36]. This mechanism ultimately leads to sensor offset-voltage drift and a slight sensitivity increase. Referring to Fig. 6, however, the bias observed in the accelerometer outputs after the pulse is from thermal heating of the sensors. In particular, the 7264B accelerometers can have a thermal shift in the zero measurand output of  $\pm 30\text{ g}$  over a  $-18^\circ$  to  $66^\circ\text{C}$  range [38]. A peak temperature of about  $46^\circ\text{C}$  temperature rise was recorded by the thermistor present in the shot depicted by Fig. 6, which means the  $-1\text{g}$  and  $+2\text{g}$  biased readings were well within the manufacturer specifications.

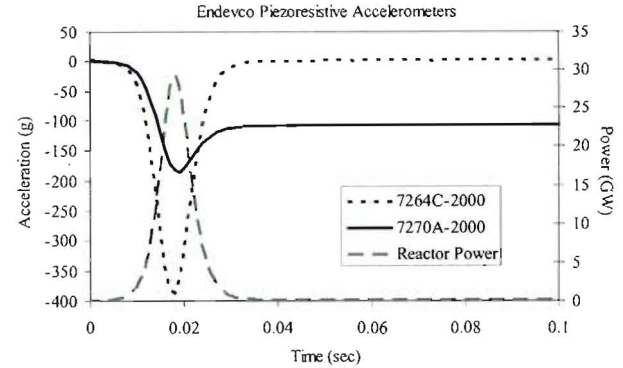


Fig. 9. Endevco piezoresistive accelerometer output after a 285-MJ ACRR pulse. The initial prompt drops by the accelerometer outputs are a radiation induced effect. The 7270A-2000 (where '-2000' denotes a 0–2000 g range) exhibits a negatively biased output after the reactor pulse.

#### V. CONCLUSIONS

Various COTS MEMS sensors being considered for use in a pulsed reactor core were operated in several different radiation environments. The performance of the Kulite pressure transducers was graphically summarized in Fig. 8, as a function of total neutron fluence and gamma dose. From Fig. 8, one can more easily observe that for neutron irradiation and lower gamma doses ( $\sim 20$  kGy), these sensors perform reasonably well. Only one sensor (an XCE-062 model) shows noticeable degradation below those levels. Otherwise, the results show promise for use of these devices (particularly, the XTE-190) in a pulsed neutron-gamma radiation environment. Survival of the Endevco piezoresistive MEMS accelerometers is observed at high neutron fluences, with the exception of a single sensor anomaly (i.e., the 7270A) at a neutron fluence of  $1.6 \times 10^{15}$  n/cm<sup>2</sup>. As compared to the Kulite pressure transducers, these accelerometers did not show signs of catastrophic failure.

We conclude that some COTS piezoresistive MEMS sensors are viable candidates for measurements in a pulsed reactor environment. We find the Kulite XTE-190 pressure transducer useable to a fluence and dose of  $4 \times 10^{15}$  n/cm<sup>2</sup> and 20 kGy, respectively. The Endevco 7264 accelerometers operate to a radiation exposure of more than twice the XTE-190. Noteworthy is that the research from this project has originated the first reported results from nuclear radiation effects testing of piezoresistive MEMS accelerometers and pressure transducers [39,40].

Although some researchers are advocating the use of MEMS devices in harsh radiation environments, we nevertheless find it necessary to perform hardness assurance testing of such sensors as is common with other semiconductor components. The differences in response by sensors from same manufacturer have been noted herein, for example, the softness of the Endevco 7270A accelerometer versus the 7264, and similarly, the softness of the Kulite XCE-062 pressure transducer compared to the XTE-190.

## REFERENCES

[1] J.E. Ramus, "Radiation induced electrical transients in strain gage and temperature transducer circuits in a pulsed reactor environment," *IEEE Trans. on Nuclear Science*, vol. 11, no. 5, Nov. 1964, pp. 111-122.

[2] C.S. Smith, "Piezoresistance effect in germanium and silicon," *Physical Review*, vol. 94, no. 1, April 1954, pp. 42-49.

[3] L.M. Roylance, J.B. Angell, "A batch-fabricated silicon accelerometer," *IEEE Trans. Electron Devices*, vol. 26, Dec. 1979, pp. 1911-1917.

[4] H. Eren, "Acceleration, Vibration, and Shock Measurement," *The Measurement, Instrumentation, and Sensors Handbook*, J. G. Webster, ed., Boca Raton: CRC Press, 1999, p. 17-14.

[5] J. Thomas, R. Kühnhold, R. Schnupp, H. Ryssel, "A silicon vibration sensor for tool state monitoring working in the high acceleration range," *Sensors and Actuators A*, vol. 85, no. 1-3, Aug. 2000, pp. 194-201.

[6] G.L. Davis, P.L. Walter, "Determining the kinematics of the Mars Pathfinder Lander from accelerometer data," *Sensors*, vol. 15, no. 1, Jan. 1998, pp. 28-35.

[7] R. Whittier, "Sensors pumped up with silicon technology," *InTech*, vol. 45, no. 9, Sept. 1998, pp. 40-42.

[8] A.D. Kurtz, A.V. Bemis, T. Nunn, A. Ned, "Method for fabricating a high pressure piezoresistive transducer," U.S. Patent 5,702,619, Dec. 30, 1997.

[9] A.D. Kurtz, A.A. Ned, S. Goodman, A.H. Epstein, "Latest ruggedized high temperature high temperature piezoresistive transducers," NASA 2003 Propulsion Measurement Sensor Development Workshop, Huntsville, AL, May 13-15, 2003, 19 pp.

[10] J.T. Suminto, "A wide frequency range, rugged silicon microaccelerometer with overrange stops," *IEEE Ninth Annual International Workshop on Micro Electro Mechanical Systems*, San Diego, CA, Feb. 11, 1996, pp. 180-185.

[11] L.P. Schanwald, J.R. Schwank, J.J. Sniegowski, D.S. Walsh, N.F. Smith, K.A. Peterson, M.R. Shaneyfelt, P.S. Winokur, J.H. Smith, B.L. Doyle, "Radiation effects on surface micromachined comb drives and microengines," *IEEE Trans. on Nuclear Science*, vol. 45, no. 6, Dec. 1998, pp. 2789-2798.

[12] *MEMS Reliability Assurance Guidelines for Space Applications*, B. Stark, Ed., JPL Publication 99-1, NASA, January 1999, p. 40.

[13] K.F. Man, "MEMS reliability for space applications by elimination of potential failure modes through testing and analysis," *Proceedings of the SPIE*, vol. 3880, Sept. 1999, pp. 120-129.

[14] L.M. Miller, "MEMS for space applications," *Proceedings of the SPIE*, vol. 3680, pt. 1-2, 1999, pp. 2-11.

[15] S. Cass, "MEMS in space," *IEEE Spectrum*, vol. 38, no. 7, July 2001, pp. 56-61.

[16] X. Lafontan, F. Pressecq, F. Beaudoin, S. Rigo, M. Dardalhon, J.-L. Roux, et al., "The advent of MEMS in space," *Microelectronics Reliability*, vol. 43, no. 7, July 2003, pp. 1061-1083.

[17] S. McClure, L. Edmonds, R. Mihailovich, A. Johnston, P. Alonso, J. DeNatale, J. Lehman, C. Yui, "Radiation effects in microelectromechanical systems (MEMS): RF relays," *IEEE Trans. on Nuclear Science*, vol. 49, no. 6, Dec. 2002, pp. 3197-3202.

[18] J.R. Caffey, P.E. Kladitis, "The effects of ionizing radiation on microelectromechanical systems (MEMS) actuators: electrostatic, electrothermal, and bimorph," *Proceedings of the IEEE International Conference on Micro Electro Mechanical Systems*, Maastricht, Netherlands, Jan. 25-29, 2004, pp. 133-136.

[19] T.F. Miyahira, H.N. Becker, S.S. McClure, L.D. Edmonds, A.H. Johnston, Y. Hishinuma, "Total dose degradation of MEMS optical mirrors," *IEEE Trans. on Nuclear Science*, vol. 50, no. 6, Dec. 2003, pp. 1860-1866.

[20] A.R. Knudson, S. Buchner, P. McDonald, W.J. Stapor, A.B. Campbell, K.S. Grabowski, D.L. Kries, S. Lewis, Y. Zhao, "The effects of radiation on MEMS accelerometers," *IEEE Trans. on Nuclear Science*, vol. 43, no. 6, Dec. 1996, pp. 3122-3126.

[21] C.I. Lee, A.H. Johnston, W.C. Tang, C.E. Barnes, J. Lyke, "Total dose effects on micromechanical systems (MEMS): accelerometers," *IEEE Trans. on Nuclear Science*, vol. 43, no. 6, Dec. 1996, pp. 3127-3132.

[22] L.D. Edmonds, G.M. Swift, C.I. Lee, "Radiation response of a MEMS accelerometers: an electrostatic force," *IEEE Trans. on Nuclear Science*, vol. 45, no. 6, Dec. 1998, pp. 2779-2788.

[23] C. Barnes, A. Johnston, C. Lee, G. Swift, B. Rax, "Recent radiation effects activities at JPL: coping with COTS," *Proceedings Third ESA Electronic Components Conference (ESTEC)*, ESA SP-395, Noordwijk, The Netherlands, April 22-25, 1997, pp. 227-244.

[24] V. Boyadzhyan, J. Choma, Jr., "High temperature, high reliability integrated hybrid packaging for radiation hardened spacecraft micromachined tunneling accelerometer," *Proc. IEEE International Workshop on Integrated Power Packaging*, Chicago, IL, Sept. 17-19, 1998, pp. 79-83.

[25] S.-Y. Zhu, Y.-P. Huang, J. Wang, A.-Z. Li, S.-Q. Shen, M.-H. Bao, "Total dose radiation effects of pressure sensors fabricated on Unibond-SOI materials," *Nuclear Science and Techniques*, vol. 12, no. 3, Aug. 2001, pp. 209-214.

[26] W.R. Langdon, W.K. Bennett, W.T. Decker, W.E. Garland, "Radiation effects on piezoresistive accelerometers," *IEEE Trans. on Industrial Electronics and Control Instrumentation*, vol. 17, April 1970, pp. 99-104.

[27] R.R. Bouche, "Accelerometers for use in nuclear reactor components," presented at the Winter Annual Meeting of the American Society of Mechanical Engineers, New York, NY, December 1, 1970, *Flow-Induced Vibration in Heat Exchangers*, pp. 36-41.

[28] R.L. Thomas, "Vibration instrumentation for nuclear reactors," *Proceedings of the International Symposium on Vibration Problems in Industry*, Keswick, Cumberland, UK, April 10-12, 1973, paper no. 627.

[29] T.K. Bierney, "Instrumentation for the measurement of vibration in severe environments such as nuclear reactors," *Operation of Instruments in Adverse Environments 1976*, Institute of Physics Conference Series No. 34, 1977, J. Knight, Ed., pp. 103-116.

[30] F.D. Terry, R.L. Kindred, S.D. Anderson, "Transient Nuclear Radiation Effects on Transducer Devices and Electrical Cables," Phillips Petroleum Company, Atomic Energy Division, IDO-17103, TID-4500, November 1965, 68 pp.

[31] W.E. Chapin, J.E. Drennan, D.J. Hamman, "The Effect of Nuclear Radiation on Transducers," Battelle Memorial Institute, REIC report no. 43, TIC report no. 3, October 31, 1966, 126 pp.

[32] L.M. Choate and T.R. Schmidt, editors, *Sandia National Laboratories Radiation Facilities*, Technical Report no. SAND92-2157, 5th edition, August 1993, pp. 4-13.

[33] T.R. Schmidt, J.A. Reuscher, "Overview of Sandia National Laboratories pulse nuclear reactors," Winter Meeting of the American Nuclear Society, Washington, DC, Nov. 13-18, 1994.

[34] J.G. Kelly, T.F. Luera, L.D. Posey, "Simulation fidelity issues in reactor irradiation of electronics-reactor environments," *IEEE Trans. on Nuclear Science*, vol. 35, no. 6, Dec. 1988, pp. 1242-1247.

[35] K.E. Holbert, J. Nessel, S.S. McCready, A.S. Heger, T. Harlow, "Investigation of neutron and gamma irradiation of piezoresistive microelectromechanical accelerometers and pressure transducers," Los Alamos National Laboratory report LA-14290, June 2006.

[36] K.E. Holbert, J.A. Nessel, S.S. McCready, A.S. Heger, T.H. Harlow, "Response of piezoresistive MEMS accelerometers and pressure transducers to high gamma dose," *IEEE Transactions on Nuclear Science*, vol. 50, no. 6, Dec. 2003, pp. 1852-1859.

[37] Product data sheets for XCE-062 and XTE-190, Kulite Semiconductor Products, Inc., Leonia, NJ.

[38] Product data sheets for 7264B, 7274C and 7270A, Endevco Corporation, San Juan Capistrano, CA.

[39] S.S. McCready, T.H. Harlow, A.S. Heger, K.E. Holbert, "Piezoresistive micromechanical transducer operation in a pulsed neutron and gamma ray environment," *IEEE Radiation Effects Data Workshop*, Phoenix, AZ, July 15-19, 2002, pp. 181-186.

[40] K.E. Holbert, S.S. McCready, A.S. Heger, T.H. Harlow, D.R. Spearing, "Performance of piezoresistive and piezoelectric sensors in pulsed reactor experiments," *Proc. Fourth ANS International Topical Meeting on Nuclear Plant Instrumentation, Controls and Human-Machine Interface Technologies*, Columbus, Ohio, September 19-22, 2004.